Surgical tissue handling methods to optimize *ex vivo* fluorescence with the activatable optical probe γ-glutamyl hydroxymethyl rhodamine green

Toshiko Harada[a], **Yuko Nakamura**[a], **Kazuhide Sato**[a], **Tadanobu Nagaya**[a], **Peter L. Choyke**[a], **Yasuyuki Seto**[b], and **Hisataka Kobayashi**[a,*]

[a]Molecular Imaging Program, Center for Cancer Research, National Cancer Institute, NIH, Bethesda, MD20892, USA

[b]Department of Stomach and Esophageal Surgery, Graduate School of Medicine, The University of Tokyo, Tokyo 113, Japan

Abstract

Optical fluorescence imaging has been developed as an aid to intraoperative diagnosis to improve surgical and endoscopic procedures. Compared with other intraoperative imaging methods, it is lower in cost, has a high safety margin, is portable and easy to use. γ-glutamyl hydroxymethyl rhodamine green (gGlu-HMRG) is a recently developed activatable fluorescence probe that emits strong fluorescence in the presence of the enzyme γ-glutamy transpeptidase (GGT), which is overexpressed in many cancers, including ovarian cancer. *Ex vivo* testing is important for clinical approval of such probes. The diagnostic performance of gGlu-HMRG in fresh excised surgical specimens has been reported; however, details of tissue handling have not been optimized. In this study, we investigated four different tissue handling procedures to optimize imaging in excised tumor specimens. The fluorescence intensity time courses after the different tissue handling methods were compared. Additionally, the fluorescence positive areas were correlated with the presence of red fluorescent protein (RFP) in an RFP positive cell line as the standard of reference for cancer location. In the 'intact' groups, tumors yielded quick and homogeneous activation of gGlu HMRG. In the 'rinse' and 'cut' groups, the fluorescence intensity of the tumor was a little lower than that in the intact group. In the 'pressed' groups, however, fluorescence intensity from gGlu-HMRG was lower over the entire time course, suggesting a decrease or relocation of excreted GGT. In conclusion, we demonstrate that the method of tissue handling prior to ex *vivo* imaging with the activatable probe gGlu-HMRG has a strong influence on the signal derive from the specimen. Published 2016. This article is a U.S. Government work and is in the public domain in the USA.

---

*Correspondence to: H. Kobayashi, Molecular Imaging Program, Center for Cancer Research, National Cancer Institute, NIH, Bethesda, MD 20892, USA. Kobayash@mail.nih.gov.

Keywords

optical navigation surgery; fluorescent probe; surgical specimen; γ-glutamyl transpeptidase; ovarian cancer

1. INTRODUCTION

Intraoperative imaging is playing an increasing role in modern surgery and endoscopy. It has the potential to aid in tumor detection and in determining the status of surgical margins in real time, thus potentially improving outcomes. However, in order for these imaging methods to be successfully introduced into clinical practice, a series of orderly pre-clinical tests must be performed. After demonstrating efficacy in animal models, *ex vivo* imaging of excised human specimens is often a preliminary test prior to clinical testing.

Various real-time imaging technologies have been developed to offer intraoperative image-guided surgery and endoscopy (1). Among them, intraoperative optical fluorescence imaging offers several advantages. Optical fluorescence is highly sensitive, involves low cost equipment, generally has a high safety margin, does not utilize ionizing radiation, and is portable and relatively straightforward to use (1–3). With the increased use of optical white light cameras in operating rooms and endoscopy suites, optical fluorescence imaging can be relatively easily integrated into the workflow.

Fluorescence probes can be either 'always on' or activatable, meaning that they are 'turned on' only under specific conditions. Activatable fluorescence probes are desirable because they produce very high target to background ratios (TBRs), improving sensitivity for pathology (4). However, by their nature, they are more complex to test as fluorescence depends on both the activating substance and the activatable fluorophore.

A recently developed activatable fluorescence probe, γ - glutamyl hydroxymethyl rhodamine green (gGlu-HMRG), emits strong fluorescence after activation by γ-glutamyl transpeptidase (GGT; Enzyme Commission number 2.3.2), an enzyme commonly found in the extracellular space of cancers (5,6). GGT is a membrane-bound enzyme that catalyzes the first step in the degradation of extracellular glutathione (GSH), by hydrolysis or by its transfer to a suitable acceptor. GGT expression, which is tissue specific in normal organs, can be generally upregulated under proliferative conditions, such as organogenesis and carcinogenesis (7–10). Therefore, although GGT expression is not specific for cancers, increased levels of GGT have been observed in various human tumors, including ovarian cancer (11–13). gGlu-HMRG, which cannot permeate the plasma membr*ane because of its hydrophilic*ity, is hydrolyzed when it encounters GGT, and yields the highly fluorescent product HMRG. HMRG, which is hydrophobic, can permeate the plasma membrane and enter cancer cells. The enzymatic activity of GGT is generally high enough to produce the fluorescent product within seconds to minutes after exposure to the probe (6).

Several studies have assessed the diagnostic performance of gGlu-HMRG for various cancers, and more studies are underway (5,14–16). However, because of the complexity of insuring that both GGT and gGlu-HMRG are present in the specimen, the handling of

surgical samples is important and has not yet been standardized. In this study, we compared different methods of tissue handling to determine their impact on gGlu-HMRG fluorescence, thus providing insights into the best practices for *ex vivo* testing of gGlu-HMRG.

2. EXPERIMENTAL

2.1. Reagents

gGlu-HMRG, a rapid activatable cancer-selective fluorescence imaging probe, was synthesized and used in this study. The synthesis method of gGlu-HMRG has been published (6).

2.2. Cell lines and culture

The established ovarian cancer cell lines SHIN3, which highly expresses GGT and shows strongly positive fluorescent signal with gGlu-HMRG, and OVCAR5, which moderately expresses GGT and shows positive fluorescent signal with gGlu-HMRG, were used for this study. The SHIN3 cell line was transfected with the red fluorescent protein (RFP DsRed2)-expressing plasmid (Clontech Laboratories) and served as the standard of reference for cancer cell location in tumors. All cells were grown in RPMI1640 medium (Invitrogen) containing 10% fetal bovine serum (Invitrogen), 0.03% L-glutamine, penicillin (100 U/ml), and streptomycin (100mg/ml) in tissue culture flasks in a humidified incubator at 37 °C in an atmosphere of 95% air and 5% carbon dioxide. All *in vivo* procedures were conducted in compliance with the Guide for the Care and Use of Laboratory Animal Resources (1996), US National Research Council, and approved by the local animal care and use committee. Six- to eight-week-old female homozygote athymic nude mice were purchased from Charles River (National Cancer Institute, Frederick, MD, USA). Two million cancer cells suspended in 300 μL phosphate-buffered saline (PBS) were injected intraperitoneally into each mouse. Imaging was performed 14–21 days after cell injection.

2.3. Comparison of procedures in preparing excised tumor specimens

gGlu-HMRG stock solution (containing 0.5% v/v DMSO as a co-solvent) was suspended in PBS to generate a 5 μM gGlu-HMRG solution for SHIN3-RFP tumors and a 50 μM gGlu-HMRG solution for OVCAR5 tumors. Five mice were euthanized by carbon dioxide inhalation for each cell line. Immediately after euthanasia, the mouse abdominal wall was excised, and then the abdominal cavity was exposed and the peritoneal tumors were extracted. Tumors were allocated into four groups of four tumors each (from 5 mm to 10 mm in diameter) for the following procedures (Fig. 1): (1) rinse tumors in PBS at 37 °C for 1 min, and then wipe excess PBS (PBS rinse group); (2) cut tumors, and expose the cut surface (cut group); (3) press tumors to the thickness of 1 mm (press group); (4) just drop the probe right after tumors are removed (intact group). A portable fluorescence camera specialized for gGlu-HMRG, which enables fluorescence imaging in the operating room or endoscopy suite, was utilized in sample studies (12,17). Fluorescent images were acquired using a Discovery portable fluorescence imaging system (INDEC BioSystems, Santa Clara, CA, USA), with the following filter set: band-pass filter from 450 to 490 nm for excitation light and filters from 511 to 551 nm for emission light. Tumors were placed on a non-fluorescent plate. After baseline fluorescence images of the tumors had been obtained, 5–10

μL of gGlu-HMRG solution was dropped on the surface of the tumors. Real-time fluorescence images of tumors were recorded every minute between 0 and 60 min after gGlu-HMRG administration at room temperature. The circular regions of interest (ROIs) were placed in the center of the tumor nodules, and the fluorescence intensities of the tumor nodules and backgrounds were measured. Then, the fluorescence intensities were calculated for each nodule. All fluorescence images were analyzed with ImageJ software (National Institutes of Health, Rockville, MD, USA) (http://rsbweb.nih.gov/ij/). Data are expressed as mean ± SEM from a minimum of four experiments.

2.4. Collation of gGlu-HMRG fluorescence positive areas with actual tumor lesions

To compare fluorescence positive areas with the actual tumor, an *in vivo* fluorescence study with SHIN3–RFP tumor was performed. A gGlu-HMRG stock solution (containing 0.5% v/v DMSO as a co-solvent) was suspended in PBS to generate a 5 μM gGlu-HMRG solution. Five SHIN3–RFP tumor bearing mice were euthanized by carbon dioxide inhalation. Immediately after euthanasia, the mouse abdominal wall was excised, the abdominal cavity was exposed, and the peritoneal SHIN3–RFP tumors (from 5 mm to 10 mm in diameter) were extracted. SHIN3–RFP tumors were allocated into the four groups of four tumors described above (Fig. 1). Spectral fluorescence images were acquired using the Maestro *in vivo* imaging system (CRi, Woburn, MA, USA). The following filter sets were used: for gGlu-HMRG fluorescence imaging, band-pass filters from 445 to 490 nm for excitation light and a filter over 515 nm for emission light (blue filter); for RFP fluorescence imaging, band-pass filters from 575 to 605 nm for excitation light and a filter over 645 nm for emission light (yellow filter). The tunable emission filter was automatically stepped in 10 nm increments from 500 to 600 nm for gGlu-HMRG and 600 to 800 nm for RFP at constant exposure to generate a spectral image. After a fluorescence image had been obtained with a yellow and blue filter setting, 5–10 μL of gGlu-HMRG solution was dropped on the surface of the tumors. Real-time fluorescence images with the blue filter setting were captured at 1, 10, and 60 min after gGlu-HMRG administration. The spectral fluorescence images consisted of autofluorescence spectra, and the spectra from gGlu-HMRG and RFP were then unmixed based on their spectral patterns using commercial software (Maestro; CRi).

2.5. Effect of temperature on fluorescence signal activated by enzyme using excised tumor specimens

An activatable probe targeting temperature-sensitive enzyme is not suitable for this study because the temperature of the extracted specimen decreases immediately after excision. B-galactosidase catalyzes the hydrolysis of lactose into glucose and galactose, and its enhanced enzymatic activity in primary ovarian cancers compared with normal ovaries has been reported (18,19). On the other hand, the activity of β-galactosidase at low temperature is poor (20–22). Thus, to validate the effect of temperature on fluorescence signal derived from an enzyme activatable probe, another *ex vivo* imaging study was performed using SHIN3-RFP tumors and HMRef-βGal, a β-galactosidase-activated fluorescence probe (19).

HMRef-βGal stock solution (containing 0.5% v/v DMSO as a co-solvent) was suspended in PBS to generate a 100 μM HMRef-βGal solution. Two mice were euthanized by carbon dioxide inhalation. Immediately after euthanasia, the mouse abdominal wall was excised,

and then the abdominal cavity was exposed and the small bowel mesentery with peritoneal SHIN3-RFP tumors was extracted. The small bowel mesentery with peritoneal SHIN3-RFP tumors was allocated into two groups of one sample with at least five peritoneal tumors each for the following procedures: (1) a heating pad kept at 37°C was placed under a non-fluorescent plate throughout the fluorescence imaging (with heating); (2) fluorescence imaging was performed without a heating pad (without heating). Acquisition of fluorescent images and image analysis were performed in the same manner as shown in the fluorescence study with SHIN3 tumor using gGlu-HMRG, except that the concentration and volume of HMRef-β Gal were 100 μM and 100 μL, and the time resolution of imaging was every 30 s to 30 min. Data are expressed as mean ± SEM from a minimum of five tumors.

Spectral fluorescence imaging and unmixing spectra for RFP fluorescence were performed in the same manner as shown in the fluorescence study with SHIN3-RFP tumor using gGlu-HMRG.

3. RESULTS

3.1. Comparison of procedures in preparing the specimen

Figure 2A, B shows the images and quantitative assessment of SHIN3 tumors after gGlu-HMRG was applied. In the cut and intact groups, the tumors were clearly observed rapidly and exhibited a consistent increase of fluorescence intensity. However, the fluorescence intensity of the cut group was lower than that of the intact group. The press group exhibited low fluorescence intensity during the entire observation period. The PBS rinse group demonstrated an increase in fluorescence over the first 20 min before it plateaued; however, the fluorescent signal was lower than that of the intact group, suggesting that GGT may have been washed out during rinsing.

Figure 3A, B shows the images and quantitative assessment of OVCAR5 tumors after gGlu-HMRG was applied. In the cut and intact groups, the tumors were clearly observed rapidly and exhibited a consistent increase of fluorescence intensity. The fluorescence intensity of the rinse group was a little lower than those of the cut and intact groups. The press group exhibited low fluorescence intensity during the entire observation period.

3.2. Correlation of gGlu-HMRG fluorescence positive areas with actual tumor lesions

SHIN3-RFP tumors were used to correlate gGlu-HMRG fluorescence with actual tumor lesions (Figure 4 and Supplementary Figure 1). In the cut group, a rapid and consistent increase of gGlu-HMRG fluorescence intensity was observed in tumors that corresponded to the RFP fluorescence signal throughout the time course. Additionally, the margin of the fluorescence positive area was clear, with high contrast. The press group showed low gGlu-HMRG fluorescence intensity during the entire observation period, which often was not consistent with the RFP fluorescence. In the PBS rinse group, gGlu-HMRG fluorescence signal was decreased and the margin was unclear at the early time points up to 10 min, and then became brighter with a little clearer margin on the later images (60 min). The gGlu-HMRG fluorescence signal was consistent with the RFP fluorescence signal. In the intact group, the gGlu-HMRG fluorescence signal was highest from early time points among all

groups. The late-phase fluorescent signals of intact surfaces of tumors were well matched with the RFP fluorescence signal, similar to that of the cut group (Figure 4 and Supplementary Figure 1).

3.3. Effect of temperature on fluorescence signal activated by enzyme using excised tumor specimens

Supplementary Figure 2 shows the images and quantitative assessment of peritoneal SHIN3-RFP tumors after HMRef-βGal was applied. In the group with heating, the fluorescence intensity of the tumors increased gradually. On the other hand, the fluorescence intensity of the group without heating increased gradually, but was lower than that of the group with heating during the entire observation period.

4. DISCUSSION

Among the different methods of handling the tissue for testing gGlu-HMRG, the method that entailed minimal handling (intact group) showed the most rapid and constant signal increases over time. Using SHIN3 and OVCAR5 tumors at later time points, cutting the specimen resulted in lower fluorescence compared with maintaining the specimen intact, suggesting that the probe can easily reach the surface tumor cells and uniformly distribute on the surface of the tumor, but not penetrate deeper into the tissue as is required with the cut specimen. GGT is reported to be a membrane-bound enzyme. However, we proved that the GGT was also excreted into the interstitial fluid adjacent to cells. Surfaces of intact tumors are broader than a clear cut surface because of the irregularity. Thus, gGlu-HMRG can reach more GGT on the cell surface. On the other hand, cut surfaces of tumors are smooth; therefore, deep penetration of gGlu-HMRG is needed to reach the same amount of GGT on the cut surface. Using SHIN3 and OVCAR5 tumors, the rinse group showed a lower fluorescence intensity than the intact group during the entire time course. However, the rinse group showed a similar kinetic curve to the intact specimen group. For instance, using SHIN3 tumors the intensity increased rapidly in the first 20 min and then plateaued, albeit at a lower level than with minimal handling (intact group). The fact that rinsing resulted in lower fluorescence suggests that GGT that is extracellular may be partly removed by rinsing with PBS. GGT is known to be present on the surface of various human cancer cells, yet the fraction that is excreted extracellularly is unknown. The exact function of GGT and how its presence benefits the tumor is still unclear (7). From the results, the excreted fraction of GGT, which can easily relocate after rinsing or pressing the specimen, can lead to false positives. In the press group, for instance, the fluorescence signal was the lowest, probably because the excreted fraction of GGT was squeezed out and tumor cells were spread onto a thin plane.

Good co-localization between gGlu-HMRG positive areas and the RFP positive region was shown in the cut and intact groups. The PBS rinse group showed a good co-localization between gGlu-HMRG and RFP early, but not later, 15 min after gGlu-HMRG administration. Thus, these data clearly indicate that the best approach for testing gGlu-HMRG is to use the intact surface of the tumor or a cut surface. Rinsing or pressing the specimen is not recommended. One would expect that this advice would also apply to other

enzyme activatable optical probes, as the reasons for decreased performance are likely to be the same (dilution for rinsing and reducing the extracellular space for pressing). When using the HMRef-βGal, β-galactosidase activated fluorescence probe, tumors in the group at room temperature without heating showed low fluorescence intensity compared with those in the group with heating because β-galactosidase is not active at room temperature (20–22). Thus, care should be taken when using temperature-sensitive enzyme activatable probes that might not be good candidates for *ex vivo* surgical sample studies.

Several *in vivo* and clinical studies assessing the diagnostic performance of gGlu-HMRG in various cancers have recently been reported (5,14–16,23). Among them, studies in which gGlu-HMRG was applied directly to the cut surface showed a rapid and constant increase of fluorescence intensity regardless of the type of specimen, for instance, surgically resected versus fine needle aspiration biopsy specimens (5,6,23). Surgical specimens showed clear tumor margins, so the lesions were easily identified. On the other hand, since endoscopically resected biopsy specimens are often small and distorted, clear cutting surfaces are difficult to expose. In such studies, gGlu-HMRG probes were applied to the intact specimen with success. The dynamic curves of fluorescence intensity showed a rapid increase at the early time points followed by plateauing of the signal, which was similar to the results obtained with intact specimens (5,6,15,24). Taken together, the results suggest that GGT, while apparently excreted from cancer cells, nevertheless tends to stay close to the cells after excretion. Therefore, squeezing or washing the specimen can relocate excreted GGT, resulting in decreased contrast at the tumor margin or even the risk of false positive diagnosis.

Our results indicated that equal distribution of the gGlu-HMRG applied to the surface of cancer tissue is important for acquiring stable activation of gGlu-HMRG on the cancer cell. Attention should be paid to this point when using topical application of the probe, especially without the ability to penetrate into the tissue (working only on the surface). Another problem of topical application of a probe working only on the surface of tumor is evaporation. The more time goes by, the more change of activity of the probe due to evaporation should be considered.

In conclusion, when testing enzyme activatable optical probes such as gGlu-HMRG on excised specimens it is important to either keep the specimen intact or use it on a cut surface. Rinsing or pressing the specimen is not recommended, as it decreases the intensity of gGlu-HMRG activation and may even cause false positives if the GGT is relocated outside the tumor location. Thus, the precise method of tissue handling is important for *ex vivo* testing of enzyme activatable probes.

Supplementary Material

Refer to Web version on PubMed Central for supplementary material.

REFERENCES

1. Keereweer S, Kerrebijn JD, van Driel PB, Xie B, Kaijzel EL, Snoeks TJ, Que I, Hutteman M, van der Vorst JR, Mieog JS, Vahrmeijer AL, van de Velde CJ, Baatenburg de Jong RJ, Lowik CW.

Optical image-guided surgery - where do we stand? Mol Imaging Biol 2011; 13: 199–207. doi: 10.1007/s11307-010-0373-2. [PubMed: 20617389]

2. Achilefu S Rapid response activatable molecular probes for intraoperative optical image-guided tumor resection. Hepatology 2012; 56: 1170–1173. doi:10.1002/hep.25807. [PubMed: 22736321]

3. Kobayashi H, Ogawa M, Alford R, Choyke PL, Urano Y. New strategies for fluorescent probe design in medical diagnostic imaging. Chem Rev 2010; 110: 2620–2640. doi:10.1021/cr900263j. [PubMed: 20000749]

4. Kobayashi H, Choyke PL. Target-cancer-cell-specific activatable fluorescence imaging probes: rational design and in vivo applications. Acc Chem Res 2011; 44: 83–90. doi:10.1021/ar1000633. [PubMed: 21062101]

5. Ueo H, Shinden Y, Tobo T, Gamachi A, Udo M, Komatsu H, Nambara S, Saito T, Ueda M, Hirata H, Sakimura S, Takano Y, Uchi R, Kurashige J, Akiyoshi S, Iguchi T, Eguchi H, Sugimachi K, Kubota Y, Kai Y, Shibuta K, Kijima Y, Yoshinaka H, Natsugoe S, Mori M, Maehara Y, Sakabe M, Kamiya M, Kakareka JW, Pohida TJ, Choyke PL, Kobayashi H, Urano Y, Mimori K. Rapid intraoperative visualization of breast lesions with gamma-glutamyl hydroxymethyl rhodamine green. Sci Rep 2015; 5: 12080. doi:10.1038/srep12080. [PubMed: 26165706]

6. Urano Y, Sakabe M, Kosaka N, Ogawa M, Mitsunaga M, Asanuma D, Kamiya M, Young MR, Nagano T, Choyke PL, Kobayashi H. Rapid cancer detection by topically spraying a gamma-glutamyltranspeptidase-activated fluorescent probe. Sci Transl Med 2011; 3: 110ra119. doi:10.1126/scitranslmed.3002823.

7. Corti A, Franzini M, Paolicchi A, Pompella A. Gamma-glutamyltransferase of cancer cells at the crossroads of tumor progression, drug resistance and drug targeting. Anticancer Res 2010; 30: 1169–1181. [PubMed: 20530424]

8. Hanigan MH. Gamma-glutamyl transpeptidase: redox regulation and drug resistance. Adv Cancer Res 2014; 122: 103–141. doi:10.1016/B978-0-12-420117-0.00003-7. [PubMed: 24974180]

9. Castellano I, Merlino A. γ-Glutamyltranspeptidases: sequence, structure, biochemical properties, and biotechnological applications. Cell Mol Life Sci 2012; 69: 3381–3394. doi:10.1007/s00018-012-0988-3. [PubMed: 22527720]

10. Zhang H, Forman HJ. Redox regulation of gamma-glutamyl transpeptidase. Am J Respir Cell Mol Biol 2009; 41: 509–515. doi:10.1165/rcmb.2009-0169TR. [PubMed: 19684307]

11. Hanigan MH, Frierson HF Jr, Swanson PE, De Young BR. Altered expression of gamma-glutamyl transpeptidase in human tumors. Hum Pathol 1999; 30: 300–305. [PubMed: 10088549]

12. Grimm C, Hofstetter G, Aust S, Mutz-Dehbalaie I, Bruch M, Heinze G, Rahhal-Schupp J, Reinthaller A, Concin N, Polterauer S. Association of gamma-glutamyltransferase with severity of disease at diagnosis and prognosis of ovarian cancer. Br J Cancer 2013; 109: 610–614. doi:10.1038/bjc.2013.323. [PubMed: 23921280]

13. Pompella A, De Tata V, Paolicchi A, Zunino F. Expression of gamma-glutamyltransferase in cancer cells and its significance in drug resistance. Biochem Pharmacol 2006; 71: 231–238. doi:10.1016/j.bcp.2005.10.005. [PubMed: 16303117]

14. Fujii T, Kamiya M, Urano Y. *In vivo* imaging of intraperitoneally disseminated tumors in model mice by using activatable fluorescent small-molecular probes for activity of cathepsins. Bioconjug Chem 2014; 25: 1838–1846. doi:10.1021/bc5003289. [PubMed: 25196809]

15. Sato C, Abe S, Saito Y, So Tsuruki E, Takamaru H, Makazu M, Sato Y, Sasaki H, Tanaka H, Ikezawa N, Yamada M, Sakamoto T, Nakajima T, Matsuda T, Kushima R, Kamiya M, Maeda S, Urano Y. A pilot study of fluorescent imaging of colorectal tumors using a gamma-glutamyl-transpeptidase-activatable fluorescent probe. Digestion 2015; 91: 70–76. doi:10.1159/000369367. [PubMed: 25632921]

16. Shimane T, Aizawa H, Koike T, Kamiya M, Urano Y, Kurita H. Oral cancer intraoperative detection by topically spraying a gamma-glutamyl transpeptidase-activated fluorescent probe. Oral Oncol 2016; 54: e16–e18. doi:10.1016/j.oraloncology.2015.12.003. [PubMed: 26810992]

17. Kakareka JW, McCann TE, Kosaka N, Mitsunaga M, Morgan NY, Pohida TJ, Choyke PL, Kobayashi H. A portable fluorescence camera for testing surgical specimens in the operating room: description and early evaluation. Mol Imaging Biol 2011; 13: 862–867. doi:10.1007/s11307-010-0438-2. [PubMed: 20960235]

18. Chatterjee SK, Bhattacharya M, Barlow JJ. Glycosyltransferase and glycosidase activities in ovarian cancer patients. Cancer Res 1979; 39: 1943–1951. [PubMed: 445394]

19. Asanuma D, Sakabe M, Kamiya M, Yamamoto K, Hiratake J, Ogawa M, Kosaka N, Choyke PL, Nagano T, Kobayashi H, Urano Y. Sensitive beta-galactosidase-targeting fluorescence probe for visualizing small peritoneal metastatic tumours in vivo. Nat Commun 2015; 6: 6463. doi:10.1038/ncomms7463. [PubMed: 25765713]

20. Wang GX, Gao Y, Hu B, Lu XL, Liu XY, Jiao BH. A novel cold-adapted beta-galactosidase isolated from *Halomonas* sp. S62: gene cloning, purification and enzymatic characterization. World J Microbiol Biotechnol 2013; 29: 1473–1480. doi:10.1007/s11274-013-1311-7. [PubMed: 23494630]

21. Cieslinski H, Kur J, Bialkowska A, Baran I, Makowski K, Turkiewicz M. Cloning, expression, and purification of a recombinant cold-adapted beta-galactosidase from antarctic bacterium *Pseudoalteromonas* sp. 22b. Protein Expr Purif 2005; 39: 27–34. doi:10.1016/j.pep.2004.09.002. [PubMed: 15596357]

22. Trimbur DE, Gutshall KR, Prema P, Brenchley JE. Characterization of a psychrotrophic *Arthrobacter* gene and its cold-active beta-galactosidase. Appl Environ Microbiol 1994; 60: 4544–4552. [PubMed: 7811090]

23. Kawakubo K, Ohnishi S, Hatanaka Y, Hatanaka KC, Hosono H, Kubota Y, Kamiya M, Kuwatani M, Kawakami H, Urano Y, Sakamoto N. Feasibility of using an enzymatically activatable fluorescence probe for the rapid evaluation of pancreatic tissue obtained using endoscopic ultrasound-guided fine needle aspiration: a pilot study. Mol Imaging Biol 2015. doi:10.1007/s11307-015-0898-5.

24. Mitsunaga M, Kosaka N, Choyke PL, Young MR, Dextras CR, Saud SM, Colburn NH, Sakabe M, Nagano T, Asanuma D, Urano Y, Kobayashi H. Fluorescence endoscopic detection of murine colitis-associated colon cancer by topically applied enzymatically rapid-activatable probe. Gut 2013; 62: 11791186. doi:10.1136/gutjnl-2011-301795.
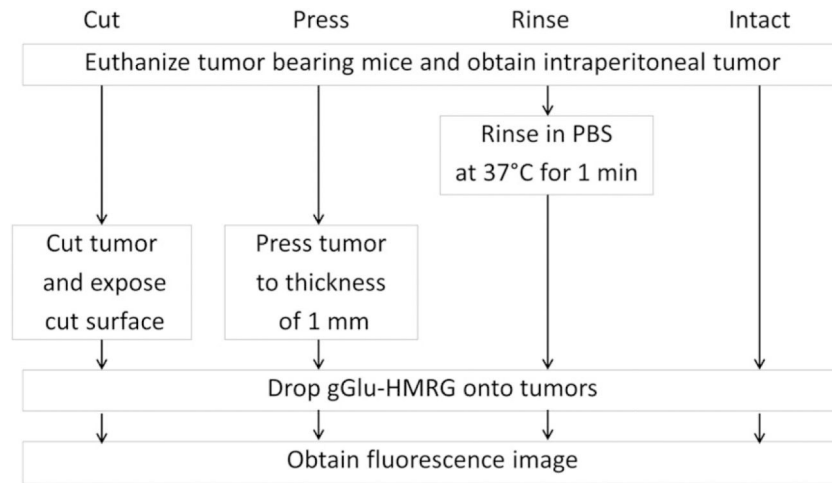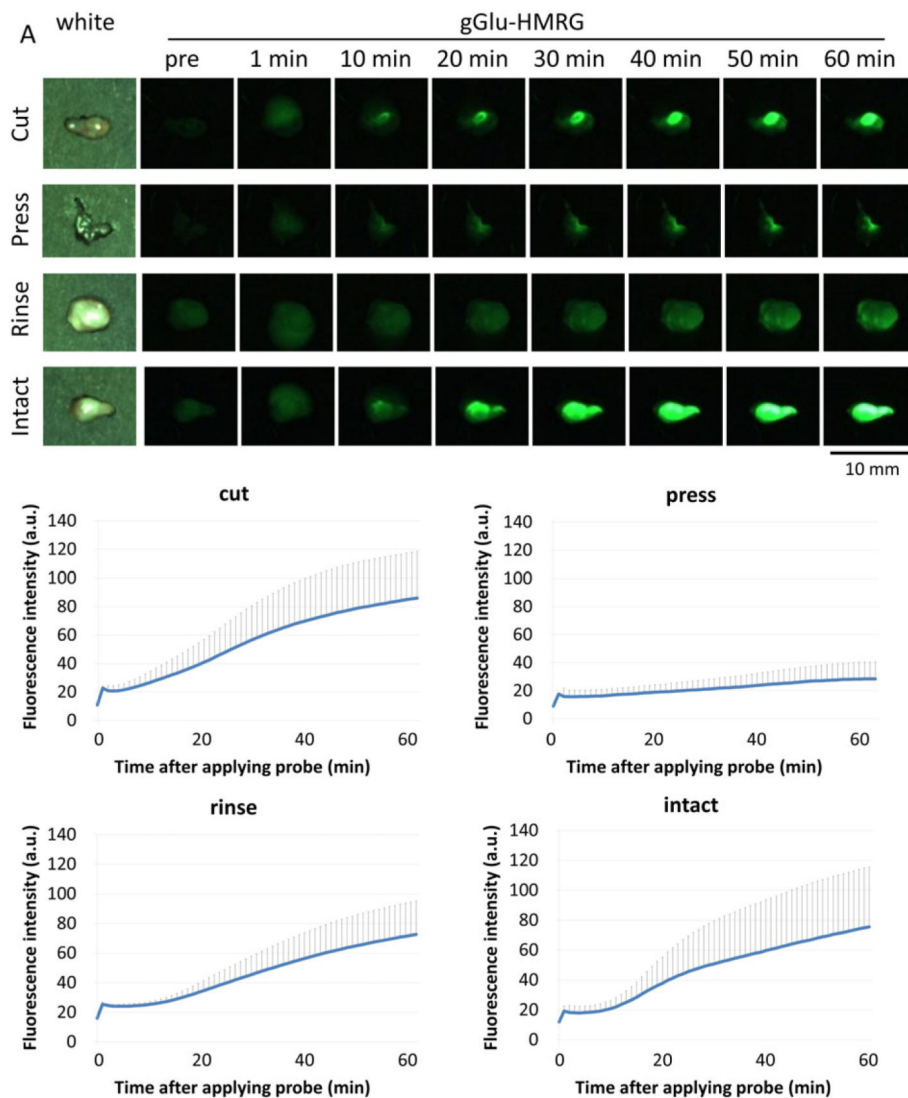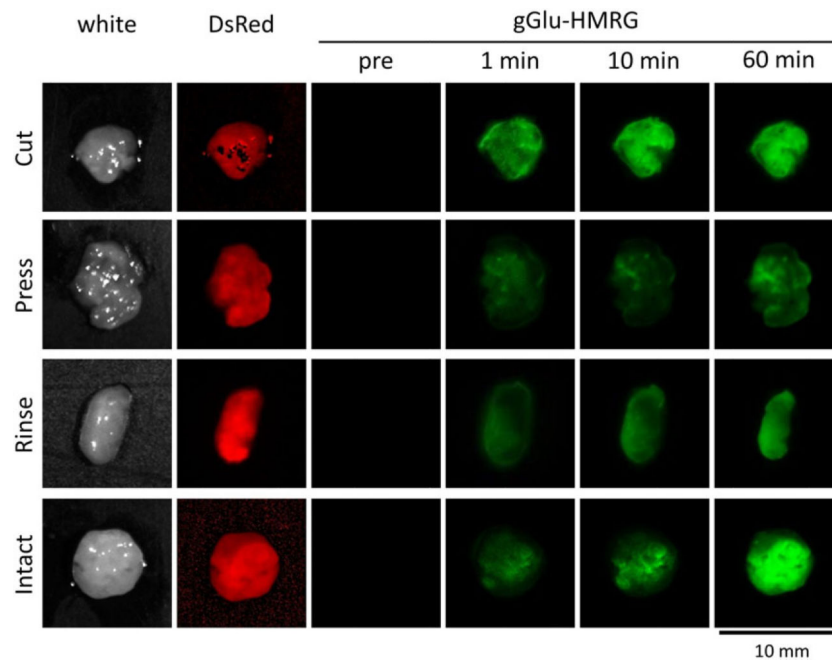
Figure 1.
Outline of study design. Groups include ($n = 4$ per group) the following: (1) rinse tumors In PBS at 37 °C for 1 min, and then wipe excess PBS (PBS rinse group); (2) cut the tumor and expose the cut surface (cut group); (3) press the tumor to the thickness of 1 mm (press group); (4) drop the probe directly on the tumor immediately after removal (intact group).
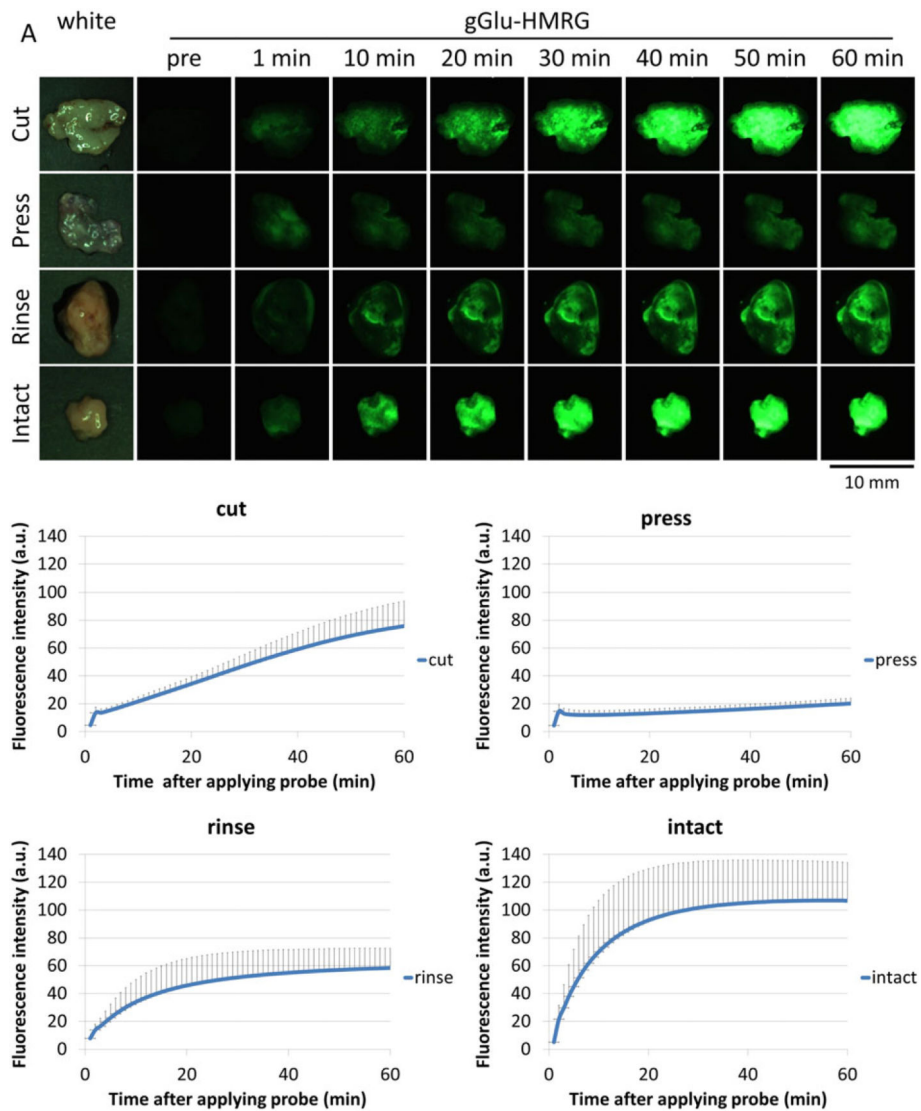
Figure 2.
gGlu-HMRG probe activation at SHIN3 tumors. (A) Representative white light and fluorescence images of SHIN3 tumors for each group (representative of four SHIN3 tumors per group) before and 1, 10, 20, 30, 40, 50, and 60 min after gGlu-HMRG administration. (B) Changes in tumor fluorescence signals in SHIN3 tumors ($n = 4$ per group). Data are mean fluorescence intensities (a.u.) $\pm$ SEM of tumors at different time points.

Figure 3.
gGlu-HMRG probe activation at OVCAR5 tumors. (A) Representative white light and fluorescence images of OVCAR5 tumors for each group (representative of four OVCAR5 tumors per group) before and 1, 10, 20, 30, 40, 50, and 60 min after gGlu-HMRG administration. (B) Changes in tumor fluorescence signals in OVCAR5 tumors ($n = 4$ per group). Data are mean fluorescence intensities (a.u.) ± SEM of tumors at different time points.

Figure 4.
gGlu-HMRG probe demonstrates fluorescence in SHIN3-RFP tumors. Representative white light images and unmixed RFP (red) and HMRG (green) fluorescence signals of SHIN3-RFP tumors for each tissue handling group (representative of four SHIN3 tumors per group) before (RFP and HMRG) and 1, 10, and 60 min after (HMRG) applying gGlu-HMRG.